Tetrahedron: *Asymmetry* 23 (2012) 1360–1368

Contents lists available at SciVerse ScienceDirect

Tetrahedron: *Asymmetry*

journal homepage: www.elsevier.com/locate/tetasy

Stereochemical preference of *Candida parapsilosis* ATCC 7330 mediated deracemization: *E*- versus *Z*-aryl secondary alcohols

Thangavelu Saravanan [a], Rajendran Selvakumar [b], Mukesh Doble [b], Anju Chadha [a,c,*]

[a] *Laboratory of Bioorganic Chemistry, Indian Institute of Technology Madras, Chennai 600 036, India*
[b] *Laboratory of Bioengineering and Drug Designing, Indian Institute of Technology Madras, Chennai 600 036, India*
[c] *National Centre for Catalysis Research, Indian Institute of Technology Madras, Chennai 600 036, India*

ARTICLE INFO

Article history:
Received 30 July 2012
Accepted 19 September 2012

ABSTRACT

The stereochemical preference of the biocatalyst, *Candida parapsilosis* ATCC 7330, was investigated with respect to the *E/Z* configuration in the deracemization and the asymmetric reduction of aryl secondary alcohols and prochiral ketones, respectively. The biocatalyst preferred the *E*-isomers over *Z*-isomers as substrates as evidenced from the experimental results of >99% ee and up to 86% isolated yield for *E*-secondary alcohols. The synthesis of enantiomerically pure *E*-4-phenylbut-3-ene-1,2-diol (ee >99%, isolated yield 86%) by whole cell mediated deracemization is reported here for the first time. The geometric preference of the enzymes was confirmed by using the cell free extract of this biocatalyst. Mechanistic insights using in silico studies showed that the *E*-isomers when located in the active site are favourably placed with respect to the catalytic triad (Ser-Tyr-Lys) for hydride transfer from NADPH.

1. Introduction

Biocatalysis or enzyme-based synthetic catalysis challenges traditional synthetic methods for producing enantiomerically pure secondary alcohols and pharmaceutical intermediates by efficiently catalysing a chemical reaction with high enantio- and regioselectivity.[1] Contrary to chemical synthesis, biocatalysis can be carried out under mild conditions.[2] In biocatalysis, both isolated enzymes and whole cells are used as catalysts. Compared to isolated enzymes, whole cell catalysts have the advantage of low cost, eliminating cofactor addition and regeneration. In addition, enzymes in the cellular milieu are well protected and stable as compared to pure (isolated) enzymes.[3]

The enantioselectivity of biocatalysts can be altered by various methods, including substrate modification, optimizing the reaction conditions, using enzyme specific inhibitors and also by medium and solvent engineering.[4] Slight modifications in the substrates can lead to a switch in the selectivity of the biocatalyst. In addition to chain length modification, functional group modification and substituent in the phenyl ring, the size of the substrate can also switch the selectivity of the biocatalyst.[5] Attempts to understand the enantioselectivity in particular the role of double bond geometry (*E/Z*) selectivity have rarely been carried out.[6]

Klibanov and Giannousis reported the geometric specificity of three different dehydrogenases (from yeast, horse liver and *Leuconostoc mesenteroiles*) in the reduction of *trans*- and *cis*-cinnamaldehydes.[7] These enzymes react with the *trans*-isomers 7 to 647 times faster than with the *cis*-counterparts, thereby displaying remarkable *trans*-specificity. The oxidative kinetic resolution of secondary alcohols by lyophilized cells of *Rhodococcus ruber* DSM 44541 showed stereo-discrimination between the *E*- and *Z*-configured secondary alcohols.[8] The *rac*-*E*-3-penten-2-ol was resolved with excellent enantioselectivity (*E* >100) whereas the corresponding *rac*-*Z*-4-penten-2-ol was not oxidized. Similarly, Burgess and Jennings reported the enantioselective esterification of unsaturated alcohols mediated by a lipase prepared from *Pseudomonas* sp., which showed stereo-discrimination between *E*-and *Z*-4-phenylbut-3-en-2-ol.[9] The *E*-isomer gave 50% conversion in 3 h with good enantioselectivity (*E* >20) whereas the *Z*-isomer gave 57% conversion in 64 h with poor enantioselectivity (*E* = 3). For over a decade, reports from our laboratory showed that *Candida parapsilosis* ATCC 7330 is effective for the deracemization of secondary alcohols,[10] the asymmetric reduction of aliphatic[11] and aromatic prochiral ketones[12] and imines,[13] and the resolution of N-acetylated amino esters.[14] This biocatalyst has also been used for the deracemization of *rac*-*E*-aryl secondary alcohols to give enantiomerically pure enantiomers with high ee (up to 99%) and isolated yields (up to 85%) via stereoinversion.[10] In order to better understand the stereospecificity of oxidoreductase enzymes in *C. parapsilosis* ATCC 7330, herein addresses the question of geometric preference using *E/Z*-secondary alcohols as substrates for deracemization and attempts to rationalize the experimentally observed results by in silico studies.

* Corresponding author. Tel.: +91 44 2257 4106; fax: +91 44 2257 4102.
E-mail address: anjuc@iitm.ac.in (A. Chadha).

0957-4166/$ - see front matter © 2012 Elsevier Ltd. All rights reserved.
http://dx.doi.org/10.1016/j.tetasy.2012.09.014

Table 1
Deracemization of *E*-secondary alcohols using *C. parapsilosis* ATCC 7330

Entry	Product	Reaction time (h)	Isolated yield (%)	ee[a] (%)	$[\alpha]_D^{25}$
1a	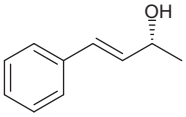	2	76	>99	+17.8 (*c* 1,MeOH)[15a]
1b	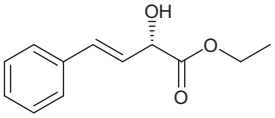	1	78	>99	+70.4 (*c* 1, $CHCl_3$)[15b]
1c	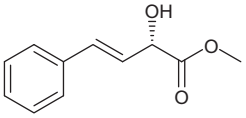	0.5	75	>99	+115.2 (*c* 1,MeOH)[15c]
1d	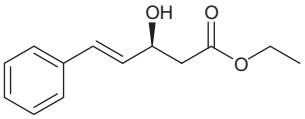	2	78	>99	−6.8 (*c* 0.5,$CHCl_3$)[10c]
1e	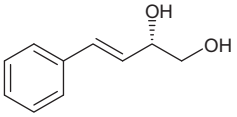	24	86	>99	+28.8 (*c* 1, $CHCl_3$)[16]

[a] Enantiomeric excess was determined using chiral HPLC columns (Chiralcel OD-H and OJ-H, flow rate 1 ml/min).

2. Results and discussion

2.1. Deracemization of *E*- and *Z*-secondary alcohols

Earlier reports from our laboratory showed that *E*-secondary alcohols were deracemized with good ee (up to >99%) using *C. parapsilosis* ATCC 7330 cells, which were harvested in the stationary phase that is 40 h.[10] Recently, culture conditions were re-optimized for the asymmetric reduction of ethyl-4-chloro-3-oxobutanoate in which *C. parapsilosis* ATCC 7330 was harvested at the mid exponential phase that is 14 h.[11] Under the newly optimized culture conditions, deracemization of *rac-E*-4-phenylbut-3-en-2-ol resulted in the corresponding enantiomerically pure (*R*)-enantiomer in excellent enantioselectivity (ee >99%) and isolated yield (76%) (Table 1, entry **1a**). The new culture conditions have the advantages of reducing the harvesting time by more than half (40 to 14 h) and doubling the substrate loading ability (from 0.97 to 2 mmol) compared to an earlier report.[10e] A variety of *rac-E*-secondary alcohols were used as substrates for deracemization to generalize the study.

The *E*-ethyl and *E*-methyl 2-hydroxy-4-phenylbut-3-enoates were deracemized using whole cells of *C. parapsilosis* ATCC 7330 to give the (*S*)-enantiomer (ee >99%) with isolated yields of 78% and 75%, respectively (Table 1, entries **1b** and **1c**). In addition, *rac-E*-ethyl 3-hydroxy-5-phenylpent-4-enoate was deracemized to the corresponding enantiomerically pure (*S*)-enantiomer with excellent enantioselectivity (>99%). Notably, the isolated yield improved from 28 to 78% compared to an earlier report (Table 1, entry **1d**).[10c] In 14 h culture conditions, the formation of a by-product (3-hydroxy-5-phenyl-pent-4-enoic acid) was not observed, unlike the reaction with the 40 h culture conditions due to the action of a hydrolase as described earlier.[10c]

Deracemization of *rac-E*-4-phenylbut-3-ene-1,2-diol was carried out using whole cells of *C. parapsilosis* ATCC 7330. Although, enantiomerically pure *E*-4-phenylbut-3-ene-1,2-diol has been synthesized by chemical methods and biocatalytic methods, this is the first report obtaining it by deracemization using a biocatalyst. Cheeseman et al. reported the palladium-catalysed, enantioselective dynamic kinetic asymmetric transformation of 3,4-epoxy-1-butene into (2*R*)-3-butene-1,2-diol (ee = 85%).[16] Cho and Shin synthesized enantiomerically pure *E*-4-phenylbut-3-ene-1,2-diol in 98% ee via a multistep oxazaborolidine-catalysed borane reduction of the corresponding β-keto sulfides.[17] Enantiomerically pure *E*- and *Z*-4-phenylbut-3-ene-1,2-diols were prepared by asymmetric dihydroxylation and hydrolytic kinetic resolution of epoxides using the chiral source 2,3-*O*-isopropylidene-D-glyceraldehyde and (*R*)-(+)-2,2-dimethyl-1,3-dioxolane-4-carboxaldehyde.[18] Aleu et al., reported the Baker's yeast mediated asymmetric reduction of an acetoxy ketone to the corresponding 1-acetoxycarbinols, which were further hydrolysed to 1,2-diols.[19] Herein the deracemization of *rac-E*-4-phenylbut-3-ene-1,2-diol to the corresponding enantiomerically pure (*S*)-enantiomer has been reported for the first time with excellent ee (>99%) and isolated yield (86%) (Table 1, entry **1e**).

Deracemization under identical reaction conditions to those used for *rac-E*-secondary alcohols was carried out with the counterpart *Z*-isomers in order to answer the question of geometric preference of this biocatalyst. The *Z*-secondary alcohols were not deracemized, indicating that the biocatalyst *C. parapsilosis* ATCC 7330 had a geometric preference towards the *E*-isomer (Scheme 1).

Recently we reported the biocatalytic deracemization of alkyl-2-hydroxy-4-arylbut-3-ynoates using the whole cells of *C. parapsilosis* ATCC 7330.[10f] The enantiomerically pure (*S,Z*)-ethyl-2-hydroxy-4-phenylbut-3-enoate **5a** was prepared via hydrogenation of the corresponding deracemized ethyl-2-hydroxy-4-phenylbut-3-ynoate **4a** using Lindlar's catalyst[20] with excellent enantiomeric excess (>99%) and good yield (94%) (Scheme 2).

2.2. Asymmetric reduction of *E*- and *Z*-4-phenylbut-3-en-2-one

Biocatalyst *C. parapsilosis* ATCC 7330 mediated the deracemization reaction by following a redox (stereoinversion) mechanism that is a two-step one-pot process that consisted of the enantioselective oxidation of one enantiomer to the keto intermediate, followed by complementary enantioselective reduction of the keto intermediate to a single enantiomer.[10] In the above deracemization

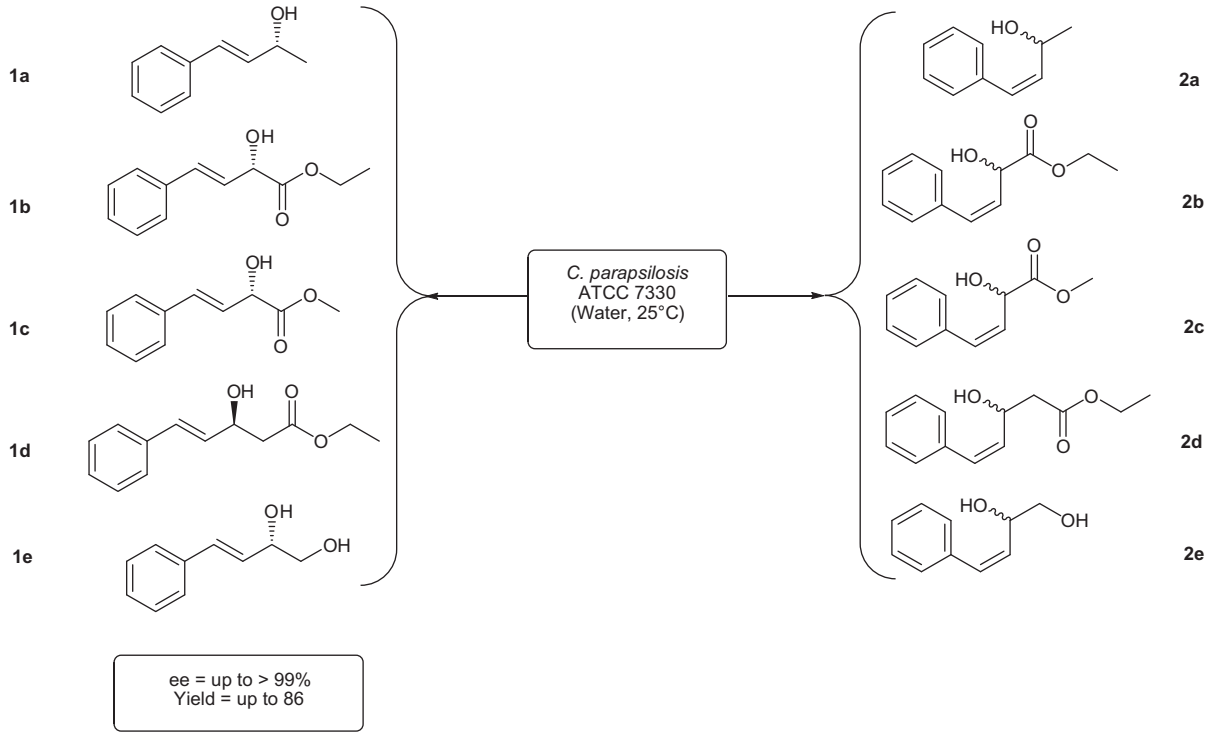

Scheme 1. Deracemization of *E*- and *Z*-4-phenylbut-3-en-2-ol derivatives.

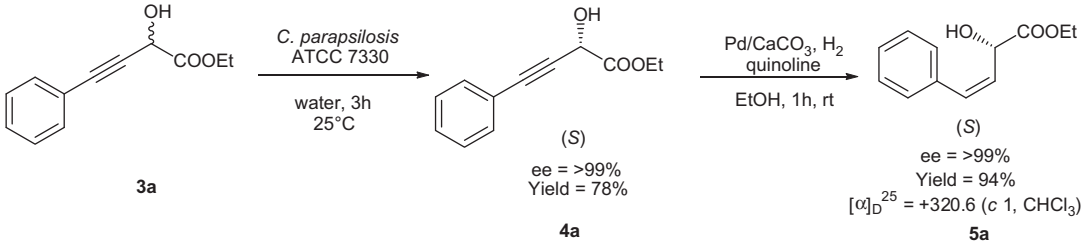

Scheme 2. Chemoenzymatic synthesis of (*S,Z*)-ethyl-2-hydroxy-4-phenylbut-3-enoate.

reactions, the stereochemical preference of the oxidizing enzyme was studied using the *E*- and *Z*-secondary alcohols as substrates. In order to study the selectivity of the reducing enzyme, *E*- and *Z*-4-phenylbut-3-en-2-ones **6a** and **7a** were synthesized and used as substrates for the asymmetric reduction.

The *E*-4-phenylbut-3-en-2-one **6a** was reduced to (*R,E*)-4-phenylbut-3-en-2-ol **6b** with excellent ee (98%) and conversion (96%). The counterpart *Z*-4-phenylbut-3-en-2-one **7a** was synthesized and subjected to asymmetric reduction under identical reaction conditions. The *Z*-ketone **7a** was not reduced, indicating that the enzyme responsible for the asymmetric reduction also shows a geometric preference towards the *E*-isomer (Scheme 3).

2.3. Dismissing role of cell membrane in substrate geometric preference

To ensure that the geometrical preference of the biocatalyst is explicitly due to the selectivity of the enzymes (oxidoreductases) and not due to the cell wall, which can influence the selectivity during the uptake of substrates, deracemization of *E*- and *Z*-4-phenylbut-3-en-2-ol was carried out using the cell free extract of *C. parapsilosis* ATCC 7330. Under these conditions, enzymes directly recruit the substrate without the cell wall barrier. As anticipated, deracemization of the *E*-isomer *rac*-**1a** gave (*R,E*)-4-phenylbut-3-en-2-ol **1a** with an ee of 98% and an isolated yield of 78% while the reaction did not progress with the *Z*-isomer *rac*-**2a**. This confirmed that the geometric preference of the biocatalyst in the deracemization is due to the enzymes and not the cell membrane.

2.4. Mechanistic insights of the geometrical specificity

The geometrical preference of *C. parapsilosis* ATCC 7330 for the asymmetric reduction was explained by modelling studies. The crystal structure of *C. parapsilosis* carbonyl reductase (CPCR) deposited in Protein Data Bank (PDB id: 3CTM)[21a] was not suitable for docking, since the cofactor binding pocket of chain A was highly collapsed and the catalytic site of chain B was completely rearranged. Hence, a model of CPCR was generated by homology modelling with the crystal structure of Mannitol Dehydrogenase (MtDH), from *Cladosporium herbarum* (PDB id: 3GDF)[21b] showing 50% sequence identity and an intact cofactor binding pocket and catalytic site. Since both 3CTM and 3GDF are short-chain dehydrogenase/reductase (SDR) family proteins, the cofactor-binding domain of the model built was expected to fold into the classical Rossmann-fold structure, a seven-strand parallel β-sheet flanked on both sides by α-helices as found in all SDR family proteins

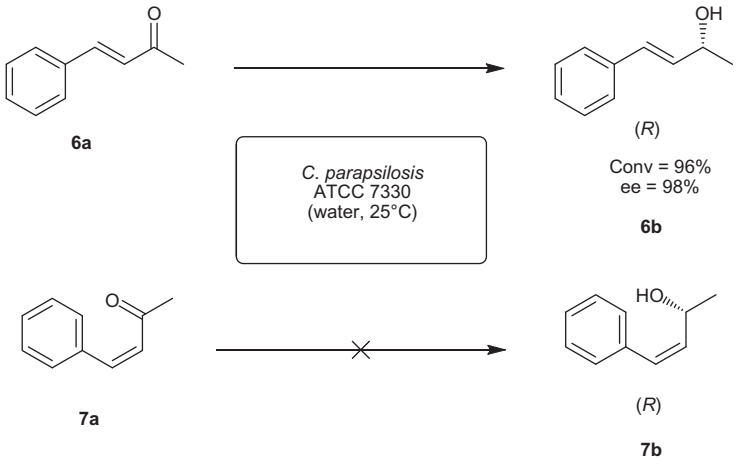

Scheme 3. Asymmetric reduction of *E*- and *Z*-4-phenylbut-3-en-2-one.

```
CPCR|B2KJ46|    MGEIESYCNKELGPLPTKAPTLSKNVLDLFSLKGKVASVTGSSG--GIGWAVAEAYAQAG 58
3GDF_A          ------------MPGQQATKHESLLDQLSLKGKVVVVTGASGPKGMGIEAARGCAEMG 46
                            :* : .*  :.:** :****** ***:**  *:*  .*.. *: *

CPCR|B2KJ46|    ADVAIWYNS--HPADEKAEHLQKTYGVHSKAYKCNISDPKSVEETISQQEKDFGTIDVFV 116
3GDF_A          AAVAITYASRAQGAEENVKELEKTYGIKAKAYKCQVDSYESCEKLVKDVVADFGQIDAFI 106
                * *** * *  : *:*:.:.*:****:::*****::.. :* *: :.:   *** **.*:

CPCR|B2KJ46|    ANAGVTWTQGPEIDVDNYDSWNKIISVDLNGVYYCSHNIGKIFKKNGKGSLIITSSISGK 176
3GDF_A          ANAGATADSG--ILDGSVEAWNHVVQVDLNGTFHCAKAVGHHFKERGTGSLVITASMSGH 164
                ****.*  .*  *  .. ::**:::.*****.::*:: :*: **:.*.***:**:*:**:

CPCR|B2KJ46|    IVNIPQLQAPYNTAKAACTHLAKSLAIEWAPFARVNTISPGYIDTDITDFASKDMKAKWW 236
3GDF_A          IANFPQEQTSYNVAKAGCIHMARSLANEWRDFARVNSISPGYIDTGLSDFVPKETQQLWH 224
                *.*:** *:.**.***.* *:*:*** **  *****:********.::**..*: :  *

CPCR|B2KJ46|    QLTPLGREGLTQELVGGYLYLASNASTFTTGSDVVIDGGYTCP 279
3GDF_A          SMIPMGRDGLAKELKGAYVYFASDASTYTTGADLLIDGGYTTR 267
                .: *:**:**::** *.*:*:**:***:***:*::******
```

Figure 1. Sequence alignment of CPCR with mannitol dehydrogenase (PDB code: 3GDF) with overall aligned score 50 using ClustalW 2.1. Notations: (∗) indicates the alignment contains identical amino acid residues in all sequences (or identical bases if protein sequences are aligned); (:) indicates the alignment contains different but highly conserved (very similar) amino acids; (.) indicates the alignment contains different amino acids that are somewhat similar and () indicates that the alignment contains dissimilar amino acids or gaps.

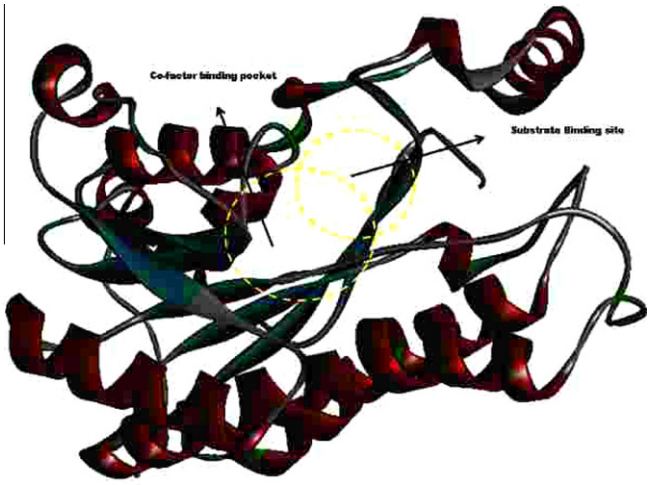

Figure 2. Structure of the modelled protein in apo form.

(Fig. 1).[21] The active site includes the Ser-Tyr-Lys catalytic triad which is located at the C-terminal end of the major parallel β-sheet. This also harbours the coenzyme- and substrate-binding pocket (Fig. 2).[22] The Ser-Tyr-Lys catalytic triad forms a proton relay system[21c] and the region is highly conserved which includes the N-terminal TGxxxGxG motif as part of the nucleotide-binding region.[23] Based on the highly conserved cofactor-binding domain, the putative enzyme-cofactor docking was performed with NADPH and NADH (Fig. 3a and b). As reported by others,[24] in both the lowest-energy conformational ensembles, the modelled domain is more favourable to NADPH (−28.01 kcal/mol) when compared to NADH (−23.54 kcal/mol). The binding energy is lower with the former than with the latter. Hence, the CPCR-NADPH complex was chosen for further docking with the *E*- and *Z*-isomers.

The docking of the co-enzyme (NADPH) with CPCR indicates that Ser43, Ile46, Tyr65, Asn66, His68, Gly120, Thr122, Val143, Tyr187 and Pro216 interact with it. Tyr187 is one among the three amino acids in the catalytic residue. Either one of the hydrides from the cofactor NADPH attacks the carbonyl carbon of the prochiral ketones from the '*Re*' or '*Si*'-face which leads to the formation

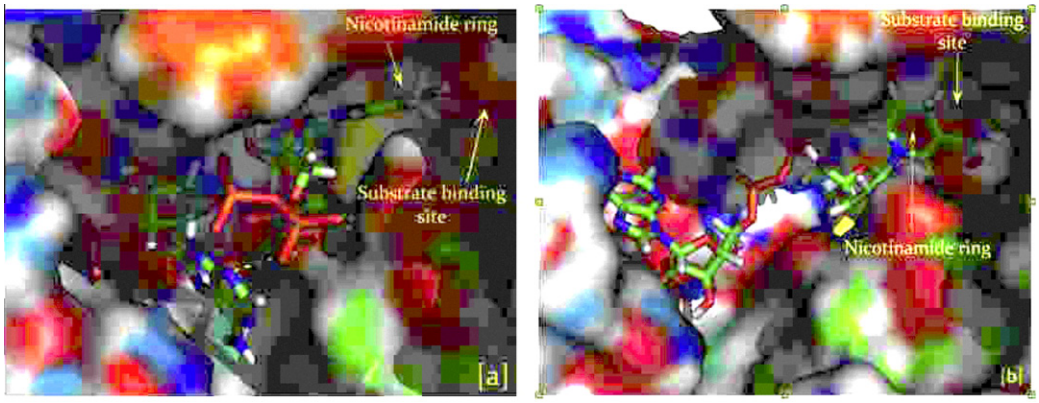

Figure 3. Structure of the modelled protein in holo form (a) NADPH bound (b) NADH bound.

Table 2
Interaction score between the substrate conformer with enzyme complex

Entry	Substrates	Scores (S)	Hydride transfer distance (Å)	Hydrogen bonding distance with TYR 187 (Å)	Absolute configuration
6a	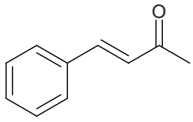	−13.97	3.68	3.21	(*R*)
7a	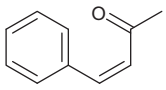	−10.26	7.67	—	—
8a	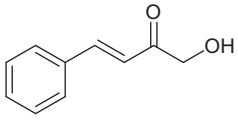	−10.35	3.72	3.70	(*S*)
9a	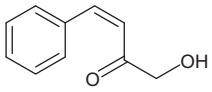	−8.52	7.89	—	—

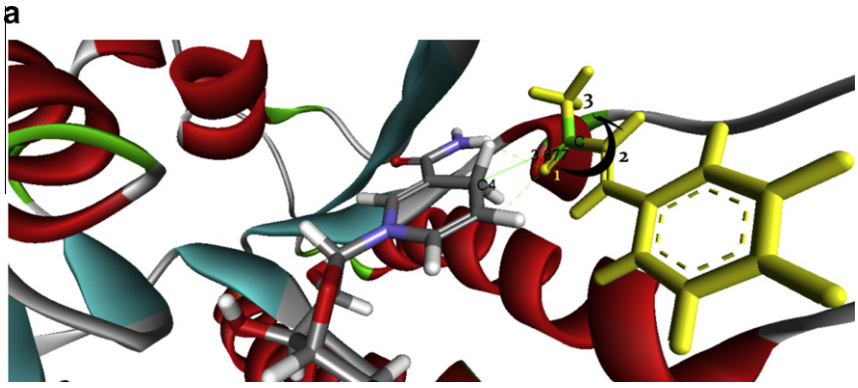

Figure 4a. Interaction of NADPH-C4 atom with *E*-4-phenylbut-3-en-2-one **6a** indicating favourable '*Si*' face attack.

of respective (*S*)- or (*R*)-alcohols.[25] For docking studies, substrates **6a** and **7a** were also used in wet lab while substrates **8a** and **9a** (*E*- and *Z*-1-hydroxy-4-phenylbut-3-en-2-one, respectively) were only studied by *in silico* methods.

It was evident from the substrate docking studies, that both **6a** and **8a** interact with the catalytic residue (Tyr187, hydroxyl group) and the NADPH-C4 atom is in close proximity to the substrates (Table 2, **6a**; 3.68 Å and **8a**; 3.72 Å) favouring a '*Si*' and '*Re*' face attack respectively, (Figs. 4a and 4b). On the other hand, neither **7a** nor **9a** is in close proximity to encounter attack from the hydride on the C4 atom of the nicotinamide ring in the cofactor (NADPH). The distances between the NADPH-C4 atom to **7a** and to **9a** are 7.67 and 7.89 Å, respectively (Table 2). The least London ΔG score[26] for CPCR-NADPH-**6a** is −13.97 kcal/mol which is lower in comparison to that of the CPCR-NADPH-**7a** complex (−10.26 kcal/mol). The lower the score, the better

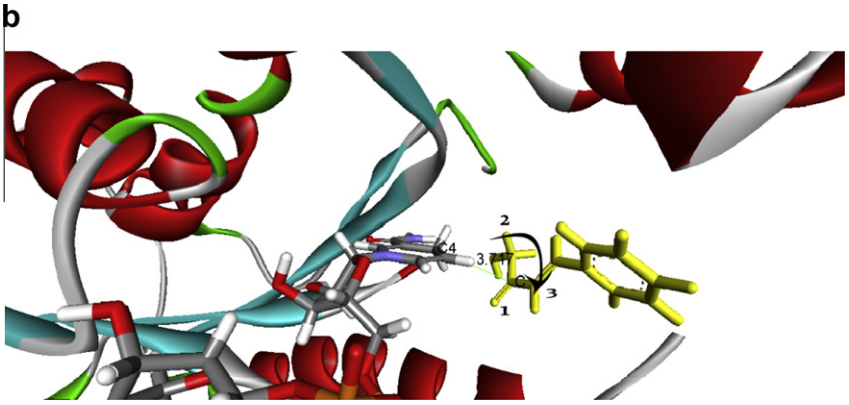

Figure 4b. Interaction of NADPH-C4 atom with *E*-1-hydroxy-4-phenylbut-3-en-2-one **8a** indicating favourable '*Re*' face attack.

the binding affinity is. Similarly, the energy of CPCR-**8a**-NAPDH complex (−10.35 kcal/mol) is less than that of the CPCR-**9a**-NADPH complex (−8.52 kcal/mol).

It should be noted that the *cis*-substrates **7a** and **9a** are away from the cofactor (7.67 and 7.89 Å, respectively), making the hydride attack difficult; therefore the product formation is not favoured (Table 2). The favourable conformation of *trans*-substrates **6a** and **8a** brings them in close proximity to the CPCR-NADPH complex to interact with the cofactor (3.68 and 3.72 Å, respectively) and allows the formation of products. It should be noted that a stereo-discrimination exists between substrates **6a** and **8a**. Although the orientation of the substrate binding to the enzyme is the same in both the cases, **6a** results in the formation of the (*R*)-enantiomer while **8a** results in an (*S*)-enantiomer due to the difference in the prioritization of the functional groups for assigning '*Re*' and '*Si*' face (Figs. 4a and 4b). Thus, the geometric preference of *C. parapsilosis* ATCC 7330 for the asymmetric reduction can be explained with the help of docking studies.

3. Conclusion

The geometric preference in the *C. parapsilosis* ATCC 7330 mediated deracemization was studied using *E*- and *Z*-secondary alcohols. It was observed that *E*-isomers were preferred over the *Z*-isomers. Enantiomerically pure *E*-secondary alcohols were synthesized *via* deracemization with excellent enantioselectivity (> 99%) and good isolated yields (up to 86%) using the 14 h culture of whole cells of *C. parapsilosis* ATCC 7330. The enantiomerically pure (*S*,*E*)-4-phenylbut-3-ene-1,2-diol (ee >99%, isolated yield 86%) was synthesized by whole cell mediated deracemization and is reported here for the first time. The geometric preference of *C. parapsilosis* ATCC 7330 was explained with the help of computational studies. The enzyme was modelled using the X-ray crystal structure of MtDH. The cofactor, NADPH, was initially docked to this modelled enzyme and then various substrates were docked to this complex. It was observed that the *E*-isomers were favourably located in the active site cavity (**6a**; 3.68 Å and **8a**; 3.72 Å) so that they could interact with the hydride of NADPH and interact with the catalytic triad. The *Z*-isomers could not achieve this proximity. Therefore, the *E*-isomers yielded the desired products while the *Z*-isomers did not.

4. Experimental

4.1. General methods

C. parapsilosis ATCC 7330 was purchased from ATCC Manassas, VA 201018, USA and maintained at 4 °C in the yeast malt agar medium that contained 5 g/L peptic digest of animal tissue, 3 g/L malt extract, 3 g/L yeast extract, 10 g/L dextrose and 20 g/L agar. The entire chemicals for media preparation were purchased locally. All chemicals used were of analytical grade and distilled prior to use. TLC was carried out on Kieselger 60 F254 aluminium sheets (Merck1.05554). Infrared spectra were recorded on a Shimadzu IR 470 instrument. ^{1}H and ^{13}C NMR spectra were recorded in $CDCl_3$ solution on a Bruker AV-400 and Bruker AVANCE III 500 MHz spectrometers. Chemical shifts are expressed in ppm values using TMS as the internal standard. Mass spectra were recorded on a Q TOF micro mass spectrometer. HPLC analysis was carried out on Jasco PU-1580 liquid chromatogram with a PDA detector using Chiralcel OD-H and OJ-H chiral columns (Daicel, 4.6*250 mm). Hexane/*iso*-propanol was used as the mobile phase. Optical rotations were determined on an Autopol-IV automatic polarimeter. The substrates *rac*-**1a-1e**,[10a,c,d] ethyl-2-hydroxy-4-phenylbut-3-ynoate **3a**[27] and methyl-2-hydroxy-4-phenylbut-3-ynoate **3b**[27] were synthesized and reported in earlier studies.

4.2. Growth conditions for *C. parapsilosis* ATCC 7330[11]

C. parapsilosis ATCC 7330 was grown in the yeast malt broth medium (50 ml) in 250 ml Erlenmeyer flasks incubated at 25 °C, 200 rpm. The cells were harvested by centrifuging the 14th hour culture broth at 10,000 rpm for 10 min at 4 °C and subsequent washing with distilled water. The process was repeated twice, and the wet cells were used for biotransformation.

4.3. Typical procedure for the deracemization of *rac-E-* and *Z*-secondary alcohols using the whole cells of *C. parapsilosis* ATCC 7330[10]

To a 250 ml conical flask containing 50 g of harvested *C. parapsilosis* ATCC 7330 cells suspended in 100 ml of sterile distilled water and 296 mg (2 mmol) of *rac-E*-4-phenylbut-3-en-2-ol *rac*-**1a** dissolved in 6 ml of ethanol as co-solvent were added. The reaction was carried out in a water bath shaker at 200 rpm and 25 °C for 2 h. After incubation, the product formed was isolated using ethyl acetate and the organic layer was dried over anhydrous sodium sulfate. The solvent was removed by evaporation and enantiomerically pure (*R*,*E*)-4-phenylbut-3-en-2-ol **1a** was obtained as a pale yellow liquid after purification by silica gel column chromatography using hexane/ethyl acetate (90:10) as the mobile phase eluent. The *ee* was found to be >99%, as determined using HPLC. The yield of the isolated product was 76%. Spectroscopic data were identical to that reported in the literature.[10d] The rest of *rac-E*- and *Z*-secondary alcohols were used as substrates for the deracemization under the same reaction conditions (Table 1). Control experiments

were done in parallel without the whole-cells under identical conditions.

4.4. Typical procedure for asymmetric reduction of *E*- and *Z*-4-phenylbut-3-en-2-one using the whole cells of *C. parapsilosis* ATCC 7330[11,12]

To a 250 ml conical flask containing 50 g of harvested *C. parapsilosis* ATCC 7330 cells suspended in 100 ml of sterile distilled water and 146 mg (1 mmol) of *E*-4-phenylbut-3-en-2-one **6a** dissolved in 3 ml of 2-propanol as co-solvent were added. The reaction was carried out in a water bath shaker at 200 rpm and 25 °C for 2 h. After incubation, the product formed was isolated using ethyl acetate and the organic layer was dried over anhydrous sodium sulfate. The solvent was removed by evaporation and enantiomerically pure (*R,E*)-4-phenylbut-3-en-2-ol **6b** was obtained as a pale yellow liquid after purification by silica gel column chromatography using hexane/ethyl acetate (90:10) as a mobile phase eluent. The ee was found to be >99%, as determined using HPLC. The yield of the isolated product was 76%. Spectroscopic data were identical to those reported in the literature.[10d] The *Z*-4-phenylbut-3-en-2-one **7a** was used as a substrate under the same conditions (Scheme 2). Control experiments were done in parallel without the whole cells under identical conditions.

4.5. Preparation of the cell free extract by cell disruption using a sonicator[28]

Harvested cells (32 g of wet cells) of *C. parapsilosis* ATCC 7330 were re-suspended in 50 ml of lysis buffer (20 mM potassium phosphate buffer, pH 6.8, 2 mM of PMSF). The suspension was then homogenized on ice by ultrasonication (a pulse of 1 s on and 2 s off, for 5 min, 40% amplitude). The homogenate was centrifuged at 10,000×*g* for 15 min at 4 °C to pellet the undisrupted cells and debris. The supernatant was used as the cell free extract for further experiments. Protein concentration (2.4 mg/ml) in the cell free extract was estimated by the Bradford method.

4.6. Deracemization *rac-E*- and *Z*-4-phenylbut-3-en-2-ol reaction using cell free extract of *C. parapsilosis* ATCC 7330

To 40 ml of cell free extract, 40 mg (0.27 mmol) of substrate *rac*-**1a** dissolved in 1 ml of DMSO was added. The reaction mixture was incubated at 25 °C for 1 h at 200 rpm. After incubation, the product formed was isolated using ethyl acetate and the organic layer was dried over anhydrous sodium sulfate. The solvent was removed by evaporation and enantiomerically pure (*R,E*)-4-phenylbut-3-en-2-ol was obtained as a colourless liquid. The *rac-Z*-4-phenylbut-3-en-2-ol *rac*-**2a** was also used as a substrate under identical reaction conditions.

4.7. Sequence alignment and homology modelling

The amino acid sequence of the carbonyl reductase was retrieved from the UniProtKB/TrEMBL database (Id: B2KJ46). NCBI's BLASTp was used to search against the protein data bank (PDB) for similar sequence identity. Among the numerous homologous sequences obtained as hits, *mannitol dehydrogenase* from *Cladosporium herbarum* (PDB Code: 3GDF) with a resolution of 2.5 Å was chosen as the template based on high sequence identity. The overall aligned score using ClustalW 2.1 was 50%.[29] The resulting template was used to model the 3D structure of *C. parapsilosis* carbonyl reductase (CPCR). The homology modelling was carried out against the chosen template using the Swiss Model.[30]

4.7.1. Structure validation

After building the protein 3D structure, in order to assess the overall stereochemical quality of the modelled protein, Ramachandran plot analysis was performed using the programme PROCHECK.[31] The ProSA[32] test was applied to the final model in order to check the energy criteria in comparison with the potential mean force derived from a large set of known protein structures. To assess the reliability of the modelled structure of CPCR, we further calculated the root mean square deviation (RMSD); this was calculated by superimposing it on the template structure (3GDF) using PYMOL. The RMSD value of the modelled CPCR protein based on the approach was 0.074 Å.

4.7.2. Docking and simulation

The Molecular Operating Environment (MOE, version 2011.10) software was used for all computations. MMFF94x force field[33] was applied for energy minimization on CPCR and substrates. The modelled CPCR enzyme structure was fixed whereas the cofactor structure (NADPH) was assumed to be flexible during these enzyme-cofactor dockings. While performing the docking with the substrates, they were considered to be flexible but the enzyme-cofactor complex was maintained rigid. The London ΔG score was calculated for all of the substrate-NADPH complexes in the CPCR enzyme. This score estimates the free energy of binding of a ligand for a given pose. The functional form of the energy term is given below

$$G = c + E_{flex} + \sum_{h-bonds} C_{HB} f_{HB} + \sum_{m-lig} C_M f_M + \sum_{atomsi} \Delta D_i$$

where, *c* represents the average gain/loss of rotational and translational entropies. Eflex is the energy due to the loss flexibility of the Ligand (calculated from Ligand topology only, f_{HB} measures geometric imperfections of hydrogen bonds and takes a value in (0,1), C_{HB} is the energy of an ideal hydrogen bond, f_M measures geometric imperfections of metal ligations and takes a value in (0,1), C_M is the energy of an ideal metal ligation and D_i is the desolvation energy of atom i. Visualization, analysing and modelling were performed using Discovery Studio Visualizer 2.5.5.[34]

4.8. Synthesis of the substrates

The substrates *E*-4-phenylbut-3-en-2-one **6a**,[35] ethyl 3-hydroxy-5-phenylpent-4-ynoate **3c**,[36] 4-phenylbut-3-yn-2-ol **3d**[37] and 4-phenylbut-3-yn-2-one **10a**[38] were synthesized as reported in the literature.

4.8.1. Synthesis of *E*-4-phenylbut-3-ene-1,2-diol *rac*-1e and 4-phenylbut-3-yne-1,2-diol 3e[27]

The Ethyl-2-oxo-4-phenylbut-3-enoate (622 mg, 3 mmol) was treated with ethanol (10 ml) in the presence of $NaBH_4$ (228 mg, 6 mmol) and $CeCl_3.7H_2O$ (1.6 g, 4.5 mmol) at room temperature. The reaction was monitored by TLC and after completion, excess alcohol was removed under vacuum. The reaction mixture was quenched with dilute HCl and extracted with dichloromethane (DCM). The organic layer was dried, concentrated, purified by silica-gel column chromatography and afforded 4-phenylbut-3-yne-1,2-diol (320 mg, 64%). The same procedure was used for the synthesis of 4-phenylbut-3-yne-1,2-diol.

4.8.2. General procedure for the synthesis of *Z*-Secondary alcohols *rac*-2a-2e and *Z*-4-phenylbut-3-en-2-one 7a[20]

Ethyl-2-hydroxy-4-phenylbut-3-ynoate (408 mg, 2 mmol) was treated with Lindlar's catalyst (180 mg) and quinoline (0.01 mmol) in ethanol (6 ml) under a nitrogen atmosphere. The nitrogen was then replaced by hydrogen gas and stirred at room temperature. The reaction was monitored by TLC. After completion of reaction,

the reaction mixture was filtered through Celite and the filtrate was concentrated. The residue was dissolved in ethyl acetate and washed with dilute HCl and then water. The organic layer was dried, concentrated and purified by silica gel column chromatography (387 mg, 94%). The same procedure was used for the synthesis of other substrates.

4.9. Spectroscopic characterization of substrates

4.9.1. *E*-4-Phenylbut-3-ene-1,2-diol[16]

^{1}H NMR (500 MHz, $CDCl_3$): δ = 2.37 (1H, br s), 2.61 (1H, br s), 3.60 (1H, dd, J = 11.5 and 7.5 Hz), 3.75 (1H, dd, J = 11.5 and 3.5 Hz), 4.44 (1H, dd, J = 9.5 Hz and 6.5 Hz) 6.19 (1H, dd, J = 16 Hz and 6.5 Hz), 6.68 (d, 1H, J = 16), 7.23–7.27 (1H, m), 7.30–7.33 (2H, m), 7.36–7.39 (2H, m); ^{13}C NMR (125 MHz, $CDCl_3$): 66.5, 73.2, 126.5, 127.7, 127.9, 128.6, 132.1, 136.3. The compound was resolved by HPLC analysis at 25 °C, using a CHIRALCEL OD-H column [hexanes/2-propanol = 90:10, 1.0 mL/min; retention times 13.0 (*S*), 14.8 min (*R*)].

4.9.2. *E*-4-Phenylbut-3-en-2-one[35]

^{1}H NMR (400 MHz, $CDCl_3$): δ = 2.38 (3H, s), 6.71 (1H, d, J = 16.4 Hz), 7.39–7.41 (3H, m), 7.51 (1H, d, J = 16.4 Hz), 7.54–7.56 (2H, m); ^{13}C NMR (100 MHz, $CDCl_3$): 27.6, 127.2, 128.4, 129.1, 130.7, 134.5, 143.6, 198.6.

4.9.3. Ethyl 3-hydroxy-5-phenylpent-4-ynoate[36]

^{1}H NMR (500 MHz, $CDCl_3$): δ = 1.29 (3H, t, J = 7.5 Hz), 2.83–2.84 (2H, m), 3.23(1H, d, J = 6 Hz), 4.21 (2H, q, J = 7 Hz), 4.99 (1H, dd, J = 12 Hz and 6 Hz) 7.28–7.32 (3H, m), 7.41–7.43 (2H, J = 2H); ^{13}C NMR (125 MHz, $CDCl_3$): 14.2, 42.0, 59.3, 61.0, 87.0, 88.0, 122.2, 128.2, 128.6, 131.7, 171.53.

4.9.4. 4-phenylbut-3-yn-2-ol[37]

^{1}H NMR (500 MHz, $CDCl_3$): δ = 1.55 (3H, d, J = 6.5 Hz), 2.13 (1H, d, J = 4.5) 4.73–4.78 (1H, m), 7.28–7.32 (3H, m), 7.41–7.44 (2H, m); ^{13}C NMR (125 MHz, $CDCl_3$): 24.3, 58.8, 84.0, 90.9, 122.6, 128.2, 128.4, 131.6.

4.9.5. 4-Phenylbut-3-yn-2-one[38]

^{1}H NMR (500 MHz, $CDCl_3$): δ = 2.45 (3H, s), 7.36–7.40 (2H, m), 7.43–7.47 (1H, m), 7.55–7. 58 (2H, m); ^{13}C NMR (125 MHz, CDCl3): 32.7, 88.2, 90.3, 119.9, 128.6, 130.7, 133.0, 184.6.

4.9.6. *Z*-Ethyl 2-hydroxy-4-phenylbut-3-enoate[39]

^{1}H NMR (500 MHz, $CDCl_3$): δ = 1.32 (3H, t, J = 7.5 Hz), 3.13 (1H, d, J = 5 Hz), 4.27–4.31 (2H, m), 5.04 (1H, dd, J = 5 Hz and 0.5 Hz), 5.64 (1H, dd, J = 11 Hz and 9.5 Hz), 6.81 (1H, d, J = 11 Hz), 7.29–7.32 (1H, m), 7.35–7.39 (2H, m), 7.44 (1H, d, J = 7.5 Hz); ^{13}C NMR (125 MHz, $CDCl_3$): 14.1, 62.2, 67.3, 127.3, 127.7, 128.3, 128.9, 134.7, 135.7, 173.9; The compound was resolved by HPLC analysis at 25 °C, using a CHIRALCEL OD-H column [hexanes/2-propanol = 90:10, 1.0 mL/min; retention times 6.0 (*R*), 8.4 min (*S*)].

4.9.7. *Z*-Methyl 2-hydroxy-4-phenylbut-3-enoate[40]

^{1}H NMR (500 MHz, $CDCl_3$): δ = 3.13 (1H, d, J = 5 Hz), 3.84 (3H, s), 5.06 (1H, m), 5.65 (1H, dd, J = 11 Hz and 9.5 Hz), 6.82 (1H, d, J = 11 Hz), 7.29–7.33 (1H, m), 7.35–7.39 (2H, m), 7.42–7.44 (1H, m); ^{13}C NMR (125 MHz, $CDCl_3$): 53.0, 67.2, 127.0, 127.8, 128.3, 128.8, 134.8, 135.6, 174.3; The compound was resolved by HPLC analysis at 25 °C, using a CHIRALCEL OD-H column (hexanes/2-propanol = 90:10, 1.0 mL/min; retention times 6.7 and 9.9 min).

4.9.8. *Z*-Ethyl 3-hydroxy-5-phenylpent-4-enoate

^{1}H NMR (400 MHz, $CDCl_3$): δ = 1.26 (3H, t, J = 7.2 Hz), 2.61 (2H, m), 3.15 (1H, br s), 4.14–4.20 (2H, m), 4.95–5.00 (1H, m) 5.70 (1H, dd, J = 11.6 and 9.2 Hz), 6.59 (1H, d, J = 11. 6 Hz), 7.25–7.37 (5H, m); ^{13}C NMR (100 MHz, $CDCl_3$): 14.3, 41.4, 61.0, 64.6, 127.6, 128.5, 128.9, 131.1, 132.1, 136.4, 172.5; IR (ν, cm^{-1}):3444, 3060, 2982, 2854, 2404, 1728, 1373, 1028, 758, 701, 669; HRMS: m/z, Calculated Mass: 243.0997 [$(M+Na)^+$], Found: 243.0990 [$(M+Na)^+$]. The compound was resolved by HPLC analysis at 25 °C, using a CHIRALCEL OD-H column (hexanes/2-propanol = 90:10, 1.0 mL/min; retention times 5.8 and 11.2 min).

4.9.9. *Z*-4-Phenylbut-3-en-2-ol[38]

^{1}H NMR (500 MHz, $CDCl_3$): δ = 1.37 (3H, d, J = 6 Hz), 1.55 (1H, bs) 4.76–4.82 (1H, m), 5.70 (1H, dd, J = 11.5 Hz and 9 Hz), 6.45 (1H, d, J = 11.5 Hz), 7.26–7.28 (3H, m), 7.33–7.36 (2H, m); ^{13}C NMR (125 MHz, $CDCl_3$): 21.6, 64.2, 127.2, 128.3, 128.8, 130.1, 135.6, 136.2. The compound was resolved by HPLC analysis at 25 °C, using a CHIRALCEL OJ-H column (hexanes/2-propanol = 95:05, 1.0 mL/min; retention times 7.7 and 9.3 min).

4.9.10. *Z*-4-Phenylbut-3-ene-1,2-diol[16]

^{1}H NMR (500 MHz, $CDCl_3$): δ = 2.58 (2H, br s), 3.59 (1H, dd, J = 11.5 and 8 Hz), 3.71 (1H, dd, J = 11.5 and 3.5 Hz), 4.67–4.70 (1H,m) 5.64 (1H, dd, J = 11.5 Hz and 9 Hz), 6.63 (d, 1H, J = 11.5), 7.25–7.29 (3H, m), 7.32–7.36 (2H, m); ^{13}C NMR (125 MHz, $CDCl_3$): 66.2, 68.7, 127.5, 128.4, 128.6, 129.6, 133.2, 136.2. The compound was resolved by HPLC analysis at 25 °C, using a CHIRALCEL OD-H column (hexanes/2-propanol = 90:10, 1.0 mL/min; retention times 9.3 and 11.9 min).

4.9.11. *Z*-4-Phenylbut-3-en-2-one[41]

^{1}H NMR (400 MHz, $CDCl_3$): δ = 2.14 (3H, s), 6.17 (1H, d, J = 12.4 Hz), 6.89 (1H, d J = 12.4 Hz), 7.34–7.36 (3H, m), 7.46–7.48 (2H, m); ^{13}C NMR (100 MHz, $CDCl_3$): 30.8, 128.3, 128.5, 129.2, 129.4, 134.1, 140.1, 201.0.

Acknowledgments

Thangavelu Saravanan thanks the Indian Institute of Technology (IIT) Madras and the University Grants Commission, India, for the fellowship. We thank the Department of Biotechnology, New Delhi, India for funding, Sophisticated Analytical Instrumentation Facility (SAIF) and Department of Chemistry, IIT Madras for NMR and mass analysis.

References

1. (a) Gotor, V. *Org. Process Res. Dev.* **2002**, *6*, 420–426; (b) Straathof, A. J. J.; Panke, S.; Schmid, A. *Curr. Opin. Biotechnol.* **2002**, *13*, 548–556; (c) Panke, S.; Wubbolts, M. *Curr. Opin. Chem. Biol.* **2005**, *9*, 188–194; (d) Pollard, D. J.; Woodley, M. J. *Trends Biotechnol.* **2007**, *25*, 66–73; (e) Jaeger, K. E.; Eggert, T. *Curr. Opin. Biotechnol.* **2004**, *15*, 305–313.
2. (a) Turner, N. J. *Nat. Chem. Biol.* **2009**, *5*, 567–573; (b) Fox, R. J.; Clay, M. D. *Trends Biotechnol.* **2009**, *27*, 137–140; (c) Rozzell, J. D. *Bioorg. Med. Chem.* **1999**, *7*, 2253–2261.
3. (a) Patel, R. N. *Microb. Technol.* **2002**, *31*, 804–826; (b) Patel, R. N. *Curr. Opin. Drug Discovery Dev.* **2003**, *6*, 902–920; (c) Ishige, T.; Honda, K.; Shimizu, S. *Curr. Opin. Chem. Biol.* **2005**, *9*, 174–180.
4. (a) Bornscheuer, U. T. *Curr. Opin. Biotechnol.* **2002**, *13*, 543–547; (b) Nakamura, K.; Yamanaka, R.; Matsuda, T.; Harada, T. *Tetrahedron: Asymmetry* **2003**, *14*, 2659–2681; (c) Kaliaperumal, T.; Kumar, S.; Gummadi, S. N.; Chadha, A. *Biocatal. Biotransform.* **2011**, *29*, 262–270; (d) Nakamura, K.; Kawai, Y.; Nakajima, N.; Ohno, A. *J. Org. Chem.* **1991**, *56*, 4778–4783; (e) Kaliaperumal, T.; Kumar, S.; Gummadi, S. N.; Chadha, A. *Tetrahedron: Asymmetry* **2011**, *22*, 1548–1552; (f) Rotthaus, O.; Kruger, D.; Demuth, M.; Shcaffner, K. *Tetrahedron* **1997**, *53*, 935–938.
5. (a) Shieh, W. R.; Gopalan, A. S.; Sih, C. J. *J. Am. Chem. Soc.* **1985**, *107*, 2994–2995; (b) Ferraboschi, P.; Grisenti, P.; Manzocchi, A.; Santaniello, E. *J. Chem. Soc., Perkin Trans. 1* **1990**, 2469–2474; (c) Wei, Z. L.; Lin, G. Q.; Li, Z. Y. *Bioorg. Med. Chem.* **2000**, *8*, 1129–1137; (d) Musa, M. M.; Fjeld, K. I. Z.; Vieille, C.; Zeikus, J. G.; Phillips, R. S. *J. Org. Chem.* **2007**, *72*, 30–34.
6. (a) Enders, D.; Jaeger, K. E. *Asymmetric Synthesis with Chemical and Biological Methods*; Willey-VCH GmbH KgaA: Weinheim, 2007. pp 399–401; (b) Zhu, D.; Yang, Y.; Buynak, J. D.; Hua, L. *Org. Biol. Chem.* **2006**, *4*, 2690–2695; (c) Cundari,

T. R.; Dinescu, A.; Zhu, D.; Hua, L. *J. Mol. Model.* **2007**, *13*, 685–690; (d) Choi, Y. H.; Choi, H. J.; Kim, D.; Uhm, K. N.; Kim, H. K. *Appl. Mocrobiol. Biotechnol.* **2010**, *87*, 185–193; (e) Jung, J.; Park, H. J.; Uhm, K. N.; Kim, D.; Kim, H. K. *Biochim. Biophys. Acta* **2010**, *1804*, 1841–1849; (f) Jakoblinnert, A.; Bocola, M.; Bhattacharjee, M.; Steinsiek, S.; Dulat, M. B.; Schwaneberg, U.; Schumacher, M. B. A. *ChemBioChem* **2012**, *13*, 803–809.
7. Klibanov, A. M.; Giannousis, P. P. *Proc. Natl. Acad. Sci. U.S.A.* **1982**, *79*, 3462–3465.
8. Stampfer, W.; Kosjek, B.; Faber, K.; Kroutil, W. *Tetrahedron: Asymmetry* **2003**, *14*, 275–280.
9. Burgess, K.; Jennings, L. D. *J. Am. Chem. Soc.* **1991**, *113*, 6129–6139.
10. (a) Baskar, B.; Pandian, N. G.; Priya, K.; Chadha, A. *Tetrahedron* **2005**, *61*, 12296–12306; (b) Padhi, S. K.; Pandian, N. G.; Chadha, A. *J. Mol. Catal. B: Enzym.* **2004**, *29*, 25–29; (c) Padhi, S. K.; Chadha, A. *Tetrahedron: Asymmetry* **2005**, *16*, 2790–2798; (d) Vaijayanthi, T.; Chadha, A. *Tetrahedron: Asymmetry* **2007**, *18*, 1077–1084; (e) Titu, D.; Chadha, A. *Tetrahedron: Asymmetry* **2008**, *19*, 1698–1701; (f) Saravanan, T.; Chadha, A. *Tetrahedron: Asymmetry* **2010**, *21*, 2973–2980.
11. Kaliaperumal, T.; Gummadi, S. N.; Chadha, A. *J. Ind. Microbiol. Biotechnol.* **2010**, *37*, 159–165.
12. (a) Baskar, B.; Pandian, N. G.; Priya, K.; Chadha, A. *Tetrahedron: Asymmetry* **2004**, *15*, 3961–3966; (b) Mahajabeen, P.; Chadha, A. *Tetrahedron: Asymmetry* **2011**, *22*, 2156–2160.
13. Vaijayanthi, T.; Chadha, A. *Tetrahedron: Asymmetry* **2008**, *19*, 93–96.
14. Stella, S.; Chadha, A. *Tetrahedron: Asymmetry* **2010**, *21*, 457–460.
15. (a) Akai, S.; Hanada, R.; Fujiwara, N.; Kita, Y.; Egi, M. *Org. Lett.* **2010**, *12*, 4900–4903; (b) Fadnavis, N. W.; Radhika, K. R.; Madhuri, K. V. *Tetrahedron: Asymmetry* **2004**, *15*, 549–553; (c) Denmark, S. E.; Fan, Y. *J. Org. Chem.* **2005**, *70*, 9667–9676.
16. Cheeseman, N.; Fox, M.; Jackson, M.; Lennon, I. C.; Meek, G. *Proc. Natl. Acad. Sci. U.S.A.* **2004**, *101*, 5396–5399.
17. Cho, B. T.; Shin, S. H. *Tetrahedron* **2005**, *61*, 6959–6966.
18. (a) Chen, J.; Lin, G. Q.; Wang, Z. M.; Liu, H. Q. *Synlett* **2002**, 1265–1268; (b) Bose, D. S.; Reddy, A. V. N.; Srikanth, B. *Synthesis* **2008**, 2323–2326; (c) Wang, F. D.; Yue, J. M. *Synlett* **2005**, 2077–2079; (d) Tiecco, M.; Testaferri, L.; Bagnoli, L.; Terlizzi, R.; Temperini, A.; Marini, F.; Santi, C.; Scarponi, C. *Tetrahedron: Asymmetry* **2004**, *15*, 1949–1955.
19. Aleu, J.; Fronza, G.; Fuganti, C.; Perozzo, V.; Serra, S. *Tetrahedron: Asymmetry* **1998**, *9*, 1589–1596.
20. Furstner, A.; Grela, K.; Mathes, C.; Lehmann, C. W. *J. Am. Chem. Soc.* **2000**, *112*, 11799–11805.
21. (a) Zhang, R.; Zhu, G.; Zhang, W.; Cao, S.; Ou, X.; Li, X.; Bartlam, M.; Xu, Y.; Zhang, X. C.; Rao, Z. *Protein Sci.* **2008**, *17*, 1412–1423; (b) Nuss, D.; Goettig, P.; Magler, I.; Denk, U.; Breitenbach, M.; Schneider, P. B.; Brandstetter, H.; Nobbe, B. S. *Biochimie* **2010**, *92*, 985–993; (c) Liese, A.; Karutz, M.; Kamphuis, J.; Wandrey, C.; Kragl, U. *Biotechnol. Bioeng.* **1996**, *51*, 544–550; (d) Oppermann, U.; Filling, C.; Hult, M.; Shafqat, N.; Wu, X.; Lindh, M.; Shafqat, J.; Nordling, E.; Kallberg, Y.; Persson, B. *Chem. Biol. Interact.* **2003**, *143*, 247–253.
22. Lesk, A. M. *Curr. Opin. Struct. Biol.* **1995**, *5*, 775–783.
23. Horer, S.; Stoop, J.; Mooibroek, H.; Baumann, U.; Sassoon, J. *J. Biol. Chem.* **2001**, *276*, 27555–27561.
24. Nie, Y.; Xiao, R.; Xu, Y.; Montelione, G. T. *Org. Biomol. Chem.* **2011**, *9*, 4070–4078.
25. Matsuda, T.; Yamanaka, R.; Nakamura, K. *Tetrahedron: Asymmetry* **2009**, *20*, 513–557.
26. MOE (The Molecular Operating Environment), 2011.10. 1010 Sherbrooke Street West, Suite 910, Montreal, Canada H3A 2R7, Chemical Computing Group Inc.; 2009.
27. Saravanan, T.; Chadha, A. *Synth. Commun.* **2011**, *41*, 2350–2358.
28. Agarwal, P. B.; Pandit, A. B. *Biochem. Eng. J.* **2003**, *15*, 37–45.
29. Larkin, M. A.; Blackshields, G.; Brown, N. P.; Chenna, R.; McGettigan, P. A.; McWilliam, H.; Valentin, F.; Wallace, I. M.; Wilm, A.; Lopez, R.; Thompson, J. D.; Gibson, T. J.; Higgins, D. G. *Bioinformatics* **2007**, *23*, 2947–2948.
30. (a) Schwede, T.; Kopp, J.; Guex, N.; Peitsch, M. C. *Nucleic Acids Res.* **2003**, *31*, 3381–3385; (b) Arnold, K.; Bordoli, L.; Kopp, J.; Schwede, T. *Bioinformatics* **2006**, *22*, 195–201.
31. Laskowski, R. A.; MacArthur, M. W.; Moss, D.; Thornton, J. M. *J. Appl. Crystallogr.* **1993**, *26*, 283–291.
32. (a) Sippl, M. J. *Proteins* **1993**, *17*, 355–362; (b) Wiederstein, M.; Sippl, M. J. *Nucleic Acids Res.* **2007**, *35*, 407–410.
33. Halgren, T. A. *J. Comput. Chem.* **1996**, *17*, 490–519.
34. Accelrys Software Inc.; Discovery Studio Modelling Environment, Release 3.1., San Diego: Accelrys Software Inc.; **2011**.
35. Bellaoued, M.; Majdi, A. *J. Org. Chem.* **1993**, *58*, 2517–2522.
36. Ramalho, R.; Jervis, P. J.; Kariuki, B. M.; Humphries, A. C.; Cox, L. R. *J. Org. Chem.* **2008**, *73*, 1631–1634.
37. Zhang, X.; Lu, Z.; Fu, C.; Ma, S. *Org. Biomol. Chem.* **2009**, *7*, 3258–3263.
38. Hamed, O.; Henry, P. M.; Becker, D. P. *Tetrahedron Lett.* **2010**, *51*, 3514–3517.
39. Aikawa, K.; Hioki, Y.; Mikami, K. *J. Am. Chem. Soc.* **2009**, *131*, 13922–13923.
40. Mikami, K.; Wakabayashi, H.; Nakai, T. *J. Org. Chem.* **1991**, *56*, 4337–4339.
41. Augustin, M. V.; Alexakis, A. *Eur. J. Org. Chem.* **2007**, 5852–5860.